A Virtual Gravity Controller for Efficient Underactuated Biped Robots

Despoina Maligianni, Fotios Valouxis, Antonios Kantounias,
Aikaterini Smyrli* *Student Member, IEEE*, and Evangelos Papadopoulos, *Life Fellow, IEEE*

***Abstract*— This paper introduces a virtual gravity controller for underactuated biped robots. A bio-inspired model of passive bipedal walking is used as the basis for the controller's design. An analytical expression of the controller is obtained, allowing on-line implementations of the developed control scheme. Following a design modification tailored to the controller, the robot is able to reproduce its passive gait even on level-ground. The results are verified via independent high-fidelity physics simulations of the real robot's digital twin. The active robot demonstrates significant dynamic convergence to the passive model's dynamics, with only minor motorization efforts. The developed control scheme showcases robustness and energetic efficiency, and leads the way to a design-oriented approach in active biped locomotion.**

I. Introduction

Bipedal robots have concentrated immense interest over the past four decades. Bipedal locomotion has numerous advantages over wheeled locomotion, including versatility and adaptability to various terrains. Nevertheless, it poses significant technical challenges, such as controller design and energetic efficiency. In contrast to bipedal robots, bipeds occurring in nature demonstrate extraordinary energy efficiency due to their passive dynamics.

Several biped robot designs and controllers have focused on the minimization of energy consumption. A common conclusion of these studies is that gravity is of great significance in bipedal locomotion [1][2]. Passive models demonstrate stable gait on negative slopes thanks to gravity torques [3][4][5], while the energy lost at heel strike impacts is restored through the biped's descend in the gravitational field [6]. However, these *passive walkers*' motion is highly dependent on the slope and their initial conditions.

In an effort to extend the passive walkers' capabilities, various controllers have been proposed. Each passive gait corresponds to an energy level: some controllers attempt to maintain the exact energy level required for a repeated gait. As shown in [7], which introduces the notion of controlled symmetry, there exist energy shaping controllers that reproduce the gaits generated by passive walkers on any slope [8]. However, these controllers require full actuation, and are not easily applicable to real-world robots [8].

The Hybrid Zero Dynamics (HZD) approach is a popular framework for designing feedback controllers, with various applications in underactuated robots, that accomplishes stable dynamic walking, presented for the first time in [9]. The HZD method has been successfully implemented in the RABBIT [10] and MABEL robots [11]. This framework is computationally more intensive than model-based controllers, posing a challenge when adaptability is required.

Virtual gravity control, which mimics the gravitational effect to accomplish passive-like gait on different slopes also poses several difficulties. Gravitational forces are field forces, and accelerate each body of a multi-body system independently. However motors that attempt to mimic these gravitational forces in underactuated biped robots will generate equal and opposite forces between two bodies of the system. This constraint may lead to dynamic divergence and prohibit the exact replication of the passive gait.

This problem can be bypassed in fully actuated walking models. In [7], a virtual gravity controller applies torques equal to the gravitational terms in a biped without knees. A similar approach has been followed for a fully actuated biped with a torso [12]. However, the method requires full actuation of the robots, which is not the case for biped walkers.

However, underactuated dynamics play an important role in bipedal walking. Just like in nature, the upper body of bipeds is often utilized as a floating base link, that receives and counters the legs' reaction torques. An example is showcased in [13], where a PD controller is used to stabilize the torso of a biped model. In another approach, an underactuated biped model with semicircular feet and without knees accomplishes stable gait with the implementation of a passivity-inspired virtual gravity controller [14].

Motivated by the fact that gravity is the driving force of passive walkers, in this paper the *Underactuated Virtual Gravity* (UVG) controller is introduced and demonstrated for the kneed biomimetic passive biped presented in [5]. To avoid the use of any PD-type controller, which would introduce terms that would tamper with the passive dynamics we wish to conserve, the passive walker model is redesigned with the addition of a counterweight link, allowing a significant convergence of the active dynamics on level ground, to the original passive dynamics on slope. This dynamic similarity allows the underactuated biped to demonstrate a very competitive Cost of Transport (COT).

This paper consists of five sections, including the introduction. Section II analyses the development of the UVG controller. In Section III, the analytically modeled system and the application of the controller is validated via independent, high-fidelity simulations of the real robot's digital twin in MSC ADAMS. Section IV presents the results and associated discussion, while Section V concludes the paper.

*Corresponding author.

Aikaterini Smyrli and Evangelos Papadopoulos are with the Robotics Institute, Athena Research Center (e-mail: katerina.smyrli@athenarc.gr, egpapado@athenarc.gr).

All authors are also with the School of Mechanical Engineering, National Technical University of Athens.

Manuscript 1463 submitted to 2025 IEEE International Conference on Robotics and Automation (ICRA). Received September 14, 2024.

II. Controller Design

A. The passive biped

The passive biped model to be controlled has been introduced in [5] and is shown in Figure 1a. The model has two identical legs: each leg is comprised of a femoral and a tibial link, connected via a four-bar mechanism which imitates the constraints imposed on the human knee by the cruciate ligaments. Both knees are equipped with viscoelastic kneecaps to prevent knee hyperextension during walking. The two femoral links are connected through a revolute joint at the hip position H. Each tibial link is rigidly connected to the biped's biomimetic feet, the geometry of which is designed to mimic the human foot's rollover shape [15]. The feet are assumed to perform rolling without slipping during their contact with the ground.

The design parameters used in this study are presented in Table I, the footshape is defined in [15] while the 4-bar knee's parameters can be found in [5] along with a detailed model description.

The biomimetic passive biped of Fig. 1(a) performs stable passive gait in a range of negative slope angles a [5]. However, on level ground the unactuated model would fail to maintain its passive repetitive walking motion, as the energy lost with each impact would no longer be restored by the biped's descent within the gravitational field. The necessary contribution of gravity in sustaining a repetitive gait may be identified through the study of the system dynamics.

B. Dynamics of walking

The generalised coordinates of the passive model include the Cartesian coordinates of the hip joint H, x_h, y_h, the femoral angles θ_{jf} and knee angles θ_{jk}, where $j = 1, 2$ for each of the biped's legs. They comprise the generalised coordinates' vector $\mathbf{q}$:

$$\mathbf{q} = [x_h, y_h, \theta_{1f}, \theta_{1k}, \theta_{2f}, \theta_{2k}]^{\mathrm{T}} \tag{1}$$

The system dynamics for some slope angle a are described by the following set of differential and algebraic equations:

$$\mathbf{M(q)\ddot{q} + C(q,\dot{q}) + G(q},a) - \mathbf{f} = \mathbf{u} \tag{2a}$$

$$\mathbf{s(q)} = \mathbf{0} \tag{2b}$$

where $\mathbf{M_{6x6}}$ refers to the joint space inertia matrix and depends solely on the biped's configuration $\mathbf{q}$, $\mathbf{C_{6x1}}$ refers to a vector that includes Coriolis, centrifugal, and kneecap viscoelastic terms, and depends on $\mathbf{q}$, $\dot{\mathbf{q}}$, $\mathbf{G_{6x1}}$ includes the gravitational terms and depends on $\mathbf{q}$ as well as on the slope a, and $\mathbf{u_{6x1}}$ refers to the vector of any external forces and torques applied to the biped. For the passive biped, $\mathbf{u} = \mathbf{0}$.

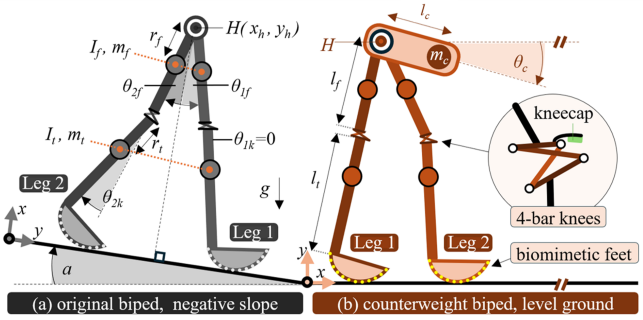

Fig. 1. (a) Bio-inspired passive biped, introduced in [15] walks down a negative slope a. (b) Biped redesign: addition of a counterweight to accommodate the UVG control and achieve level-ground walking.

TABLE I

Design Parameters of the Biped.

Parameter	Value	Parameter	Value
m_f	1.19 [kg]	I_f	0.54 $\times 10^{-2}$ [kg m^2]
m_t	0.29 [kg]	I_t	0.65 $\times 10^{-2}$ [kg m^2]
m_c	3.33 [kg]	g	9.81 [m/s^2]
l_f	0.19 [m]	r_f	0.06 [m]
l_t	0.36 [m]	r_t	0.17 [m]
l_c	0.03 [m]	r_c	0.03 [m]

The vector $\mathbf{s}$ introduces the vertical and horizontal kinematic constraints associated with the rolling motion of each foot that touches the ground. Bipedal gait consists of two phases: the single stance phase (SSP), when one only foot touches the ground, and the double stance phase (DSP), when both feet are in contact with the ground. Hence, the number of constraints in $\mathbf{s}$ changes during gait: the size of $\mathbf{s}$ is (nx1), where n $= 2$ in the SSP and n $= 4$ in the DSP.

Finally, the vector $\mathbf{f_{6x1}}$ introduces the generalized forces originating from the legs' interaction with the ground:

$$\mathbf{f} = \left(\frac{\partial \mathbf{s}}{\partial \mathbf{q}}\right)^{\mathrm{T}} \boldsymbol{\lambda} \triangleq \boldsymbol{\Lambda}(\mathbf{q})\boldsymbol{\lambda} \tag{3}$$

in which $\boldsymbol{\lambda}$ refers to the vector of Lagrangian multipliers, comprised of constraint forces in the direction of each imposed constraint in $\mathbf{s}$, and $\boldsymbol{\Lambda}$ is the constraint Jacobian. The constraint forces in $\boldsymbol{\lambda}$ constitute the Ground Reaction Forces (GRF) acting on the biped. Due to their dependency from $\mathbf{s}$ in (3), the size of $\boldsymbol{\lambda}$ is (nx1), while $\boldsymbol{\Lambda}$ is (6xn).

Eq. (2) is a system of differential and algebraic equations, with (6+n) equations and (6+n) unknowns $(\boldsymbol{\lambda}, \mathbf{q})$, with n depending on the gait phase as previously defined. It is intuitive that the GRF are not independent of the biped's state, and therefore we seek to write $\boldsymbol{\lambda}$ as a function of $(\mathbf{q}, \dot{\mathbf{q}})$ to investigate this dependency.

Firstly, we perform a double differentiation of the constraint equations of the system in (2) which yields:

$$\boldsymbol{\Lambda}^{\mathbf{T}}\ddot{\mathbf{q}} + \dot{\boldsymbol{\Lambda}}^{\mathbf{T}}\dot{\mathbf{q}} = \mathbf{0} \tag{4}$$

Next, we solve for $\ddot{\mathbf{q}}$ in (2) and substitute in (4), which allows the isolation of $\boldsymbol{\lambda}$:

$$\boldsymbol{\lambda} = -\boldsymbol{\Delta}[\dot{\boldsymbol{\Lambda}}^{\mathbf{T}}\dot{\mathbf{q}} + \boldsymbol{\Lambda}^{\mathbf{T}}\mathbf{M}^{-1}(-\mathbf{C} - \mathbf{G} + \mathbf{u})] \tag{5a}$$

$$\boldsymbol{\Delta} = (\boldsymbol{\Lambda}^{\mathbf{T}}\mathbf{M}^{-1}\boldsymbol{\Lambda})^{-1} \tag{5b}$$

As $\mathbf{M}$ is positive-definite and the Jacobian $\boldsymbol{\Lambda}$ has full column rank, with rk$(\boldsymbol{\Lambda}) = n < 6$, the matrix $(\boldsymbol{\Lambda}^{\mathbf{T}}\mathbf{M}^{-1}\boldsymbol{\Lambda})$ is (nxn) positive-definite, hence invertible in both SSP and DSP. Eq. (5) holds for both the SSP and the DSP: the size of $\boldsymbol{\lambda}$ and $\boldsymbol{\Lambda}$ changes as defined, and the operational space inertia matrix $\boldsymbol{\Delta}$ is (nxn), changing in size during gait.

Eq. (5) may be used in (2) to solve for $\ddot{\mathbf{q}}$ and obtain a 6x6 system of differential equations, having integrated the algebraic constraints through the substitution of $\boldsymbol{\lambda}$.

Most importantly, (5) demonstrates the dependence of the GRF on the model's inertial properties, gravitational field, and any input torques that may act on the biped.

Manuscript 1463 submitted to 2025 IEEE International Conference on Robotics and Automation (ICRA). Received September 14, 2024.

C. Compensating changes in gravity

As the biped passively and stably descends a downhill slope a, the gravitational torques restore the energy lost by the impacts at the heel and knee strikes [6]. For some a_*, the biped performs passive walking and $\mathbf{u_*} = \mathbf{0}$:

$$\mathbf{M\ddot{q} + C + G_* - \Lambda\lambda_* = 0} \tag{6}$$

To achieve the same walking patterns on a zero slope $a_0 = 0$, these gravitational torques must be *artificially* supplied to the biped by an external torque vector $\mathbf{u_0}$. The model's dynamics for level-ground walking are written:

$$\mathbf{M\ddot{q} + C + G_0 - \Lambda\lambda_0 = u_0} \tag{7}$$

where $\boldsymbol{\lambda_0}$ is calculated from (5) using a_0 in the calculation of $\mathbf{G}$ and $\mathbf{G_0 = G(q,}a_0\mathbf{)}$.

The goal is to find at least one $\mathbf{u_0}$ that can drive the biped to *mimic* its passive trajectory on negative slope, when walking on level ground. To exactly replicate the passive trajectory, $\mathbf{q}$, $\dot{\mathbf{q}}$ and $\ddot{\mathbf{q}}$ should be equal in (6) and (7).

Considering that the slope parameter a only affects the gravity torque vector $\mathbf{G}$, and that $\boldsymbol{\lambda}$ is a function of $\mathbf{G}$, we find that the terms containing $\mathbf{G}$ and $\boldsymbol{\lambda}$ would not be eliminated when subtracting (6) from (7):

$$\mathbf{(G_0 - G_*) + \Lambda(\lambda_* - \lambda_0) = u_0} \tag{8}$$

Using (5) to substitute $\boldsymbol{\lambda}$ and $\boldsymbol{\lambda_0}$ in (8) leads to:

$$\mathbf{(I - \Lambda\Delta\Lambda^T M^{-1})(\Gamma - u_0) = 0} \tag{9a}$$

$$\mathbf{\Gamma = G_0 - G_*} \tag{9b}$$

in which $\mathbf{\Gamma_{6x1}}$ is a *gravitational supplement* and $\mathbf{I_{6x6}}$ is the 6x6 identity matrix.

Eq. (9) defines a relationship between $\mathbf{u_0}$ and the gravitational terms one should supply to achieve level-ground walking. It also involves the biped's inertial properties and constraint Jacobian.

The existence of a $\mathbf{u_0}$ to satisfy (9) would guarantee a passivity-inspired active gait for the biped on level ground.

D. Underactuation

Eq. (9) is of the general type:

$$\mathbf{Ax = 0} \tag{10}$$

where:

$$\mathbf{A_{6x6} \triangleq I_{6x6} - \Lambda\Delta\Lambda^T M^{-1}} \tag{11a}$$

$$\mathbf{x_{6x1} \triangleq \Gamma - u_0} \tag{11b}$$

The trivial solution of (10), $\mathbf{x = 0}$ would imply:

$$\mathbf{u_0 = \Gamma} \tag{12}$$

However, the biped studied here is underactuated, as there is no way to actuate the linear DOF x_h, y_h of $\mathbf{q}$ in (1). This means that $\mathbf{u_0}$ must be of the form:

$$\mathbf{u_0} = [0, 0, u_{\theta 1 f}, u_{\theta 1 k}, u_{\theta 2 f}, u_{\theta 2 k}]^T \tag{13}$$

in which only the femoral and knee angles of the biped can be actuated. However, $\mathbf{\Gamma}$ is a 6x1 vector of non-zero elements, as $a_* \neq a_0$; hence, the trivial solution in (12) is not eligible for use in underactuated biped robots.

Eq. (10) may have other groups of solutions that lie in the null-space of $\mathbf{A}$, if $\mathbf{A}$ is not full rank.

It can be proven that $\mathrm{rk}(\mathbf{A}) = (6 - n)$ depending on the phase of the gait. (*Proof*: see the Appendix). Therefore $\mathbf{A}$ is not full rank during the biped's gait. In the passive trajectory $\mathbf{q}(\mathrm{t})$ we wish to replicate there is no DSP due to the stiffness of the legs, and therefore $\mathrm{rk}(\mathbf{A}) = 4$, $\mathrm{null}(\mathbf{A}) = 2$.

Let $\mathbf{x_1}$ and $\mathbf{x_2}$ be two vectors that span the null space of $\mathbf{A}$. For $\mathbf{x}$ in (10) to belong in the null space of $\mathbf{A}$, it must be of the form:

$$\mathbf{x} = k_1\mathbf{x_1} + k_2\mathbf{x_2} \tag{14}$$

where k_1 and k_2 are scaling parameters that can be arbitrarily selected. This would translate to the following algebraic system of 6 equations:

$$\mathbf{\Gamma - u_0} = k_1\mathbf{x_1} + k_2\mathbf{x_2} \tag{15}$$

which has a total of 6 unknowns: the 4 elements of $\mathbf{u_0}$ in (13) and the 2 scaling parameters k_1 and k_2. The solution of (15) satisfies (9) and therefore, if $\mathbf{u_0}$ is applied to the biped, it will lead to a *stable active gait on level ground*, replicating the passive trajectories of the biped on negative slope. As the system is fully defined, $\mathbf{u_0}$ is unique in achieving this gait on level ground. Consequently, it would be impossible to satisfy (15) if $\mathbf{u_0}$ contained less than 4 independent elements, as this would result in an over-defined system.

E. Biped redesign

The passive biped can achieve gait in a range of negative slopes a_*[5]. For the biped of Table I this range is $a_* \in [-0.95°, -0.45°]$, and here an intermediate value of $a_* = -0.6°$ is chosen to demonstrate the controller.

The elements $u_{\theta 1 f}$ and $u_{\theta 2 f}$ of (13) are calculated using (15) for every timestep of the biped's recorded passive trajectory, and shown in Fig. 2a.

A common approach in actuating biped robots is to use a single actuator between the two femoral links [16]. Here, this is not an option as $u_{\theta 1 f}$ and $u_{\theta 2 f}$ would have to be of equal magnitude and opposite sign. This is not the case, as depicted in Fig. 2a. In fact, it has already been shown with (15) that a gravity compensating control is not possible if $\mathbf{u_0}$ in (13) has less than 4 independent elements.

However, the negative sum of $u_{\theta 1 f}$ and $u_{\theta 2 f}$

$$u_c = -(u_{\theta 1 f} + u_{\theta 2 f}) \tag{16}$$

is observed to be almost constant throughout the biped's gait, see Fig. 2b. This leads to the redesign of the biped with the addition of a *counterweight* (CW) link at the hip, that will be used to mount the two independent femoral actuators.

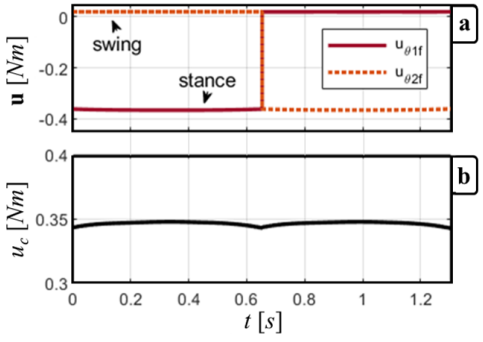

Fig. 2. (a) The femoral torques $u_{\theta 1 f}$, $u_{\theta 2 f}$ required for level-ground walking are not equal to each other. (b) The sum of reaction torques u_c is almost constant throughout the gait.

The redesigned biped is shown in Fig. 1b; it is *identical* to the passive biped with the sole addition of the CW. The newly introduced CW will be subject to the sum of reaction torques u_c in (16), which does not exhibit significant fluctuation throughout the desired trajectory as observed in Fig. 2b.

At the same time, the CW, featuring a point mass m_c at a length l_c from the hip joint and positioned at a CW angle θ_c, is subject to the gravitational torque:

$$w_c = m_c g l_c \cos(\theta_c) \tag{17}$$

where g is the acceleration of gravity. The equation governing its motion can be appended to the system dynamics:

$$(I_c + m_c l_c^2)\ddot{\theta}_c + \cancelto{0}{f_M} = u_c - w_c \tag{18}$$

where f_M is the vector containing inertial terms that describe the dynamic coupling of the CW with the rest of the biped. Eq. (18) can be simplified by assuming $f_M \approx 0$, an assumption that will be revisited during controller validation.

Ideally, to ensure that the CW does not accelerate and that $\ddot{\theta}_c \approx 0$ in (18), requires that $w_c \approx u_c$. For select m_c, l_c, this would translate to the biped maintaining a specific θ_{c*} throughout its gait, see Fig. 3a. As the CW angle is not directly controlled, the value of u_c will fluctuate and will not be exactly equal to w_c.

However, one may design the CW so that the dynamics of its motion are stable. Specifically, by placing the CW in the 4^{th} quaternion as shown in Fig. 3b, if the CW rotates below θ_{c*}, the decrease in $\cos(\theta_c)$ will cause a drop in w_c, see Fig. 3c. This will lead to $w_c < u_c$ and therefore $\ddot{\theta}_c > 0$, causing θ_c to increase and overpass θ_{c*}, resulting in $w_c > u_c$, see Fig. 3d. In this way, the motion of the CW will always be sustained within a small range of angles around θ_{c*}.

F. Underactuated Virtual Gravity (UVG) controller

Following the calculation of the torques $\mathbf{u_0}$ required to drive the level-ground biped towards its passive slope trajectory, and the subsequent redesign of the biped via the addition of the CW link, the UVG controller under development can be formulated and tested on the biped robot.

A summary of this controller is presented in Fig. 4. The original biped dynamics model of (2) is used as the base of the model-based controller. The difference between slope and

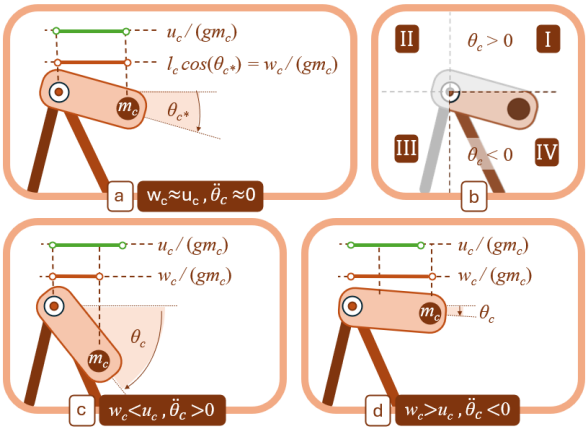

Fig. 3. CW design. (a) Ideal position of CW where gravity torque w_c equalizes the motor reaction torque u_c. (b) Positioning of the CW in the 4^{th} quaternion allows a stable CW trajectory demonstrated in (c) and (d).

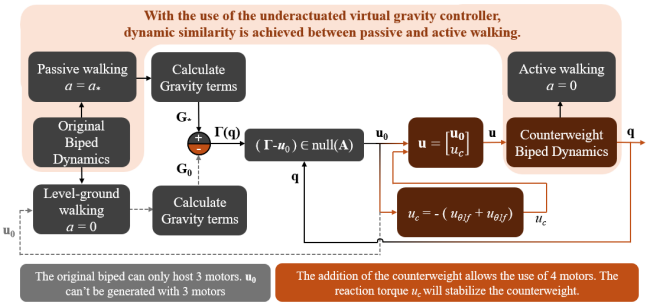

Fig. 4. Overview of the proposed UVG controller.

level-ground dynamics can be pinpointed to the contribution of gravitational torques: $\mathbf{G_*}$ in the slope and $\mathbf{G_0}$ on level ground. Their difference $\mathbf{\Gamma}$ is a function of $\mathbf{q}$. To provide this gravitational supplement, the difference $\mathbf{\Gamma - u_0}$ should lie in the null space of $\mathbf{A}$ in (10). From this, the 4 independent non-zero torque elements of $\mathbf{u}_0$ in (13) are calculated.

If the *virtual gravity* controller $\mathbf{u}_0$ were supplied to the original biped of Fig. 1a, the biped would indeed replicate its passive trajectory on level ground. However, this biped can only host 3 motors, as there are only 4 bodies that make up the biped. Therefore, the 4 non-zero terms of $\mathbf{u}_0$ cannot be supplied to the original biped of Fig. 1a.

The addition of a CW link in Fig. 1b introduces a fifth body and provides a means of hosting 4 independent motors, to actuate the original 4 rotational DOFs according to the virtual gravity requirements. The newly introduced CW DOF is designed to inherently achieve stability, under the combined effect of the femoral motor reaction torque u_c and the gravitational terms w_c that act on it.

The new system should demonstrate dynamic similarity to the original passive biped under the drive of the *underactuated virtual gravity* (UVG) controller, $\mathbf{u_{7x1}} = [\mathbf{u_0^T}, u_c]^{\mathbf{T}}$:

$$\mathbf{u} = [0, 0, u_{\theta 1 f}, u_{\theta 1 k}, u_{\theta 2 f}, u_{\theta 2 k}, -(u_{\theta 1 f} + u_{\theta 2 f})]^T \tag{19}$$

The UVG controller $\mathbf{u}$ is a *model-based* controller that is analytically evaluated at each time instance, and only requires an estimation of the model parameters and a state feedback of the generalized coordinates $\mathbf{q}$.

G. Controller validation

The analytical model of the CW biped, Fig. 1b, walking on level ground and actuated by the UVG controller is numerically simulated using Matlab. The biped converges to a steady state walking pattern which is indefinitely maintained.

Fig. 5 presents the steady state trajectory of the femoral angle of Leg 1, θ_{1f}, for the active CW biped at level ground $a = 0$, using $a_* = -0.6°$ in the UVG. The trajectory follows a clockwise progression with time. The Heel-Strike (HS) and Knee-Strike (KS) events for each of the biped's legs have been marked in the diagram. The repetitive trajectory indicates that a limit cycle has been reached for the active biped. The success of the UVG-actuated level-ground gait validates the assumptions made in the CW design phase.

Fig. 5 also presents the original passive biped's trajectory on slope a_*. The comparison reveals indistinguishable responses of the passive and active bipeds: the UVG has achieved the replication of the passive gait on level ground.

Manuscript 1463 submitted to 2025 IEEE International Conference on Robotics and Automation (ICRA). Received September 14, 2024.

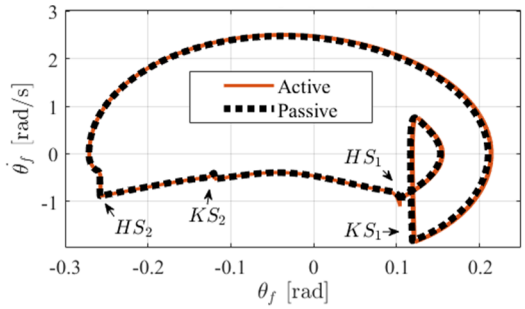

Fig. 5. Dynamic similarity of passive (slope) and active (level-ground trajectory), achieved by the UVG controller. The trajectories are almost identical. HS: Heel-Strike, KS: Knee-Strike. Due to the biped's stiffness, the Toe-Off event of one leg coincides with the contralateral HS.

III. System Validation

A. Digital Twin

The preceding analysis concerned an analytical model of the robot, simulated in Matlab. In fact, the model's parameters have been selected to match the geometric and inertial characteristics of a real-world robot design.

Specifically, a detailed CAD of the active CW robot has been designed in SolidWorks, based on the proposed biped model. The model is quasi-symmetrical around the sagittal plane, to minimize the impact of three-dimensional effects and ensure similarity with the 2D dynamics model, see Fig. 6. Fig. 6a presents the modeled femoral and tibial links, as well as the CW. The four-bar knees and biomimetic footshape geometries are also fully modeled.

To validate the developed controller, the SolidWorks model was imported in the physics simulation program MSC Adams, see Fig. 6b. The geometric and inertial parameters of the model were automatically imported from the detailed SolidWorks model. The Adams biped is an active biped, a *digital twin* of the real-world implementation of the biped model similarly to [17]. The Adams robot is controlled using the UVG controller detailed in Section II.

The simulations of the Adams robot are completely independent from the simulations of the Matlab model. As such, they can be used to evaluate the controller's design and suitability for real-world applications.

Contrarily to the simplified analytical model of Matlab, the Adams model incorporates distributed inertias and detailed ground contact modeling. The Adams model also includes the 4 motors required to control the biped's joints as well as the CW link. A tibial synchronization mechanism is added to ensure that the outer tibiae are dynamically linked. Additionally, while the Matlab model handles the four-bar knees as kinematic constraints, the Adams model introduces a detailed rigid-body dynamic representation of the mechanism. These differences are expected to cause some degree of dynamic divergence of the two models.

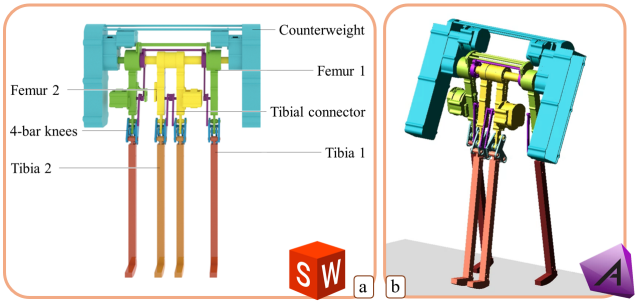

Fig. 6. (a) Detailed CAD modeling of the active CW biped in SolidWorks. (b) Physical simulations of the high-fidelity CAD model in MSC Adams.

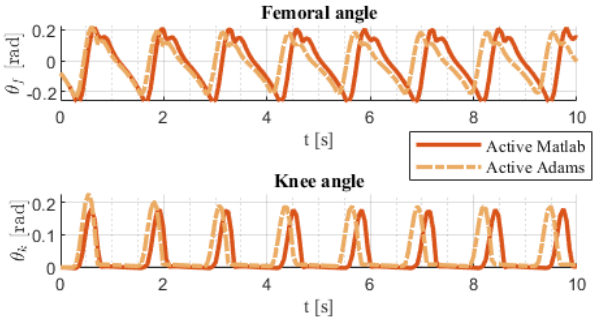

Fig. 7. Comparison of the Matlab and Adams simulations of the active CW biped using UVG control. The gait exhibited by the two models is very similar. Both models converge to a stable gait.

The controller has been designed based on the simplified Matlab model: given the differences of the two models, its successful use in the Adams model would indicate significant dynamic robustness of the developed scheme.

B. Model validation

Using MSC Adams, the CAD model is simulated for its level-ground walking using the developed UVG controller, until its convergence to a stable gait. The initial conditions provided to the Adams model are identical to the initial conditions provided to the Matlab simulation. Fig. 7 presents a comparison of the gait dynamics of the Matlab and Adams active robots under UVG control, where the femoral and tibial angles of the robots are plotted as a function of time.

The Adams model quickly converges to a stable walking trajectory. This trajectory is very similar but not identical to the one exhibited by the simplified Matlab model, which is expected given the different level of modeling detail in the two models. Notably, the Adams model exhibits a smaller step period; however, the achievement of the Adams biped's periodic gait indicates that the designed controller is robust, as it leads to a stable gait on level ground even with the aforementioned differences in model structure.

IV. Results and Discussion

The UVG controller has been shown to successfully lead to a stable gait in both the simplified Matlab model and the high-fidelity Adams model, indicating its robustness. Another significant expected advantage of the UVG controller is the small amount of energy required to sustain gait, due to the fact that it compliments a passive behavior of the robot.

Indeed, the virtual gravity controller has been designed to imitate the effects of gravity in passive walking, and as such to achieve a low energy-cost gait. In fact, the $\mathrm{COT_p}$ of *passively* walking down a slope a_* has been found in [6]:

$$\mathrm{COT_p} = |\sin(a_*)| \tag{20}$$

which is very small for the selected slope $a_* = -0.6°$, $\mathrm{COT_p} = 0.0105$. In the active robot, using the UVG controller, it is expected that $\mathrm{COT_a} \approx \mathrm{COT_p}$.

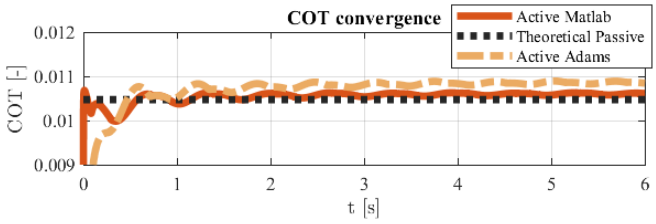

Fig. 8. Both Matlab and Adams active models converge towards the theoretical passive COT using the UVG controller.

The $\mathrm{COT_a}$ is calculated during the simulations as:

$$\mathrm{COT_a} = \frac{E_{in}}{M \cdot g \cdot \Delta x} \tag{21}$$

where E_{in} is the mechanical energy supplied through the motors, M is the total mass of the robot and Δx is the horizontal distance travelled during the gait.

As shown in Fig. 8, the $\mathrm{COT_a}$ of the active Matlab model under the virtual gravity controller quickly converges to the theoretical passive $\mathrm{COT_p}$. A slight increase of the Matlab active robot's $\mathrm{COT_a}$ is due to the assumption that there is no regenerative breaking in the motors, while the gravitational field is conservative.

The same holds for the Adams model, where an additional increase in the $\mathrm{COT_a}$ is observed due to the dynamic differences of the two models, as detailed in Section III.

Nevertheless, both active robots' COT converge close to the theoretical passive value $\mathrm{COT_p}$. The proposed UVG controller is shown to be effective in generating a sustainable, passivity-inspired stable gait in both models walking on level ground, while achieving a very low $\mathrm{COT_a}$ of under 0.011.

For the UVG controller to achieve this gait, the biped must have the ability to perform passive walking on some negative slope. This is highly dependent on design parameters: it has been shown that there are several combinations of parameters that lead to stable passive gaits in a range of slope angles [18][19]. The smaller the passive walking angle a_*, the smaller the COT using the UVG controller: bipeds that can passively walk down smaller slopes can also walk more efficiently, highlighting the importance of design optimization in walking robots. As there can be no passive walking on level ground, the design optimization process may lead to reduced $\mathrm{COT_a}$, but it will never reach zero.

Indeed, Fig. 9 presents the biped's horizontal velocity $\dot{x_h}$ and $\mathrm{COT_a}$ from (21), for various a_*. The biped can stably walk on level ground using the UVG controller with $a_* \in [-0.95°, -0.45°]$. The selection $a_* = -0.6°$ used in this paper is highlighted in the diagram. For values of a_* outside this range the biped cannot perform level-ground walking, as no stable gait exists for the passive biped on these slopes. However, it is shown that various values of a_* lead to stable gait on level ground, demonstrating the robustness of the UVG controller.

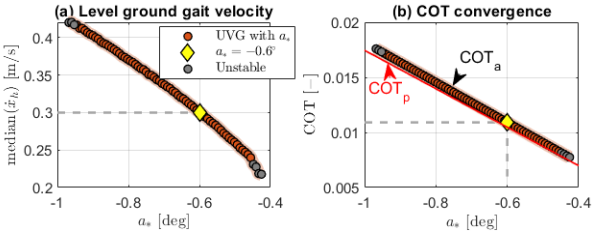

Fig. 9. Correlation of the UVG slope parameter a_* with (a) the achieved horizontal velocity, and (b) the acheived $\mathrm{COT_a}$, for level-ground walking using the UVG controller.

The choice of a_* has an important effect on the horizontal velocity of the biped as shown in Fig. 9a. The range of walking velocities for this biped using the UVG controller is $\dot{x_h} \in [0.25, 0.42] m/s$, which is significant for a biped measuring $0.55m$ in height. Decreasing a_* results to higher achieved velocities, at the expense of increased energy consumption, as shown in Fig. 9b. In all cases, the measured $\mathrm{COT_a}$ is slightly larger than the theoretical passive $\mathrm{COT_p}$ plotted with a red line, presenting significant energetic efficiency.

Overall, the proposed UVG controller has been shown to be a robust, energy-efficient option for underactuated bipedal locomotion on level ground. The same control scheme and biped robot design may be further extended to achieve an upheel gait with minor modifications. Furthermore, the proposed scheme may be applied to more complex biped robots and humanoids, as the upper body may substitute this simple model's CW. The study demonstrates the great potential of leveraging the innate passive dynamics of biped walkers in locomotive control design. Our upcoming work focuses on the manufacture of the real-world biped robot, to perform real-life experiments.

V. Conclusion

In this paper, a novel virtual gravity controller for underactuated biped locomotion has been developed. The controller was analytically derived using the dynamic model of a bio-inspired biped robot, able of passive walking on slope. The passive biped was redesigned to address the controller's stability requirements, without suppressing the passive dynamics of the walker. The method was validated using independent, high-fidelity simulations of the real-robot's digital twin. With the UVG controller, the robot demonstrated stable, robust, and energetically efficient walking on level ground.

Appendix

Here we prove that $\mathrm{rk}(\mathbf{A}) = (6 - n)$ for $\mathbf{A}$ in (11a).

- Proof that $\mathrm{rk}(\mathbf{A}) \leq (6 - n)$:
  - By right-multiplying (11a) with $\mathbf{\Lambda}$ and using (5b): $\mathbf{A\Lambda = \Lambda - \Lambda\Delta\Delta^{-1} = 0}$
  - Neither $\mathbf{A}$ nor $\mathbf{\Lambda}$ are null matrices.
  - $\mathbf{\Lambda}$ is full column rank and therefore the n independent columns of $\mathbf{\Lambda}$ are in the null-space of $\mathbf{A}$.
  - Thus, $\mathrm{null}(\mathbf{A}) \geq n$ or $\mathrm{rk}(\mathbf{A}) \leq (6 - n)$.
- Proof that $\mathrm{rk}(\mathbf{A}) \geq (6 - n)$:
  - The product $\mathbf{B = \Lambda\Delta\Lambda^T M^{-1}}$ is $\mathrm{rk}(\mathbf{B}) \leq n$, as:
    - $\mathbf{\Delta}$ and $\mathbf{M^{-1}}$ are positive-definite, and
    - $\mathrm{rk}(\mathbf{B}) \leq \min(\mathrm{rk}(\mathbf{\Lambda}), \mathrm{rk}(\mathbf{M^{-1}}), \mathrm{rk}(\mathbf{\Delta})) = n$.
  - Rewriting (11a) as $\mathbf{I = A + B}$:
    - $6 = \mathrm{rk}(\mathbf{I}) \leq \mathrm{rk}(\mathbf{A}) + \mathrm{rk}(\mathbf{B}) \leq \mathrm{rk}(\mathbf{A}) + n$
    - Therefore, $\mathrm{rk}(\mathbf{A}) \geq (6 - n)$.
- Consequently, $\mathrm{rk}(\mathbf{A}) = (6 - n)$.

REFERENCES

[1] A. Omer et al., "Study of bipedal robot walking motion in low gravity: Investigation and analysis," in *Int. Journal of Advanced Robotic Systems*, vol. 11 no. 139, 2014.

[2] A. Omer et al., "Initial Study of bipedal robot locomotion approach on different gravity levels," in *IEEE/SICE Int. Symposium on System Integration, Kyoto, Japan*,pp. 802-807, 2011.

[3] T. McGeer, "Passive walking with knees," in *Proceedings., IEEE Int. Conf. on Robotics and Automation*, vol. 3, pp. 1640-1645, 1990

[4] M. Garcia, A. Chatterjee, A. Ruina and M. Coleman,"The simplest walking model: stability, complexity, and scaling," Journal of Biomech. Eng., vol. 120 no. 2 pp. 281-288, 1998.

[5] A. Smyrli and E. Papadopoulos, "Improved biped walking performance around the kinematic singularities of biomimetic four-bar knees," *IEEE/RSJ Int. Conf. on Intelligent Robots and Systems*, Kyoto, Japan, pp. 6774-6779, 2022.

[6] A. Smyrli, M. Ghiassi, A. Kecskeméthy and E. Papadopoulos, "On the effect of semielliptical foot shape on the energetic efficiency of passive bipedal gait," *IEEE/RSJ Int. Conf. on Intelligent Robots and Systems,* Macau, China, pp. 6302-6307, 2019.

[7] A. Goswami, B. Espiau, A. Keramane, "Limit Cycles in a Passive Compass Gait Biped and Passivity Mimicking Control Laws," *Autonomous Robots*, vol 4,no 3, pp. 273-286, 1997.

[8] M.W. Spong, J.K. Holm, D. Lee, "Dynamics of Bipedal Locomotion Passivity-Based Control of Bipedal Locomotion Regulating Walking by Exploiting Passive Gaits in 2-D and 3-D Bipeds," *IEEE Robotics and Automation Mag.*, vol. 14, no. 2, pp. 30-40, 2007.

[9] E.R. Westervelt, J. W. Grizzle and D. E. Koditschek, "Hybrid zero dynamics of planar biped walkers," in *IEEE Trans. on Automatic Control*, vol. 48, no. 1, pp. 42-56, 2003.

[10] C. Chevallereau et al., "RABBIT: a testbed for advanced control theory," *IEEE Control Systems Mag.*, vol. 23, no. 5, pp. 57-79, 2003.

[11] W. Grizzle et al., "MABEL, a new robotic bipedal walker and runner," *American Control Conf.,* St. Louis, MO, USA, pp. 2030-2036, 2009.

[12] H. Sasaki and M. Yamakita, "Efficient Walking Control of Robot with Torso Based on Passive Dynamic Walking," *IEEE Int. Conf. on Mechatronics,* pp. 113-120, 2009.

[13] T. Narukawa, M. Takahashi and K. Yoshida, "Biped locomotion on level ground by torso and swing-leg control based on passive-dynamic walking," *IEEE/RSJ Int. Conf. on Intelligent Robots and Systems*, Edmonton, AB, Canada, pp. 4009-4014, 2005.

[14] A. Smyrli A, G. Bertos and E. Papadopoulos, "Efficient stabilization of zero-slope walking for bipedal robots following their passive fixed-point trajectories". *IEEE Int. Conf. on Robotics and Automation*, pp. 5733-5738, 2018.

[15] A. Smyrli and E. Papadopoulos, "A methodology for the incorporation of arbitrarily-shaped feet in passive bipedal walking dynamics," *IEEE Int. Conf. on Robotics and Automation*, pp. 8719-8725, 2020.

[16] X. Xiao, O. Ma and F. Asano, "Control walking speed by approximate-kinetic-model-based self-adaptive control on underactuated compass-like bipedal walker," *IEEE Int. Conf. on Robotics and Automation (ICRA),* , Singapore, pp. 4729-4734, 2017.

[17] Vasileiou, C., Smyrli, A., Drogosis, A. and E. Papadopoulos, "Development of a passive biped robot digital twin using analysis, experiments, and a multibody simulation environment", *Mechanism and Machine Theory*, 163, 104346, 2021.

[18] A. Smyrli, G. Bertos, and E. Papadopoulos, "A generalized model for compliant passive bipedal walking: sensitivity analysis and implications on bionic leg design," *ASME J. of Biomech. Eng.*, 143(10): 101008, 2021.

[19] A. Smyrli and E. Papadopoulos, "Modeling, Validation, and Design Investigation of a Passive Biped Walker with Knees and Biomimetic Feet," *Proc. IEEE Int. Conf. on Robotics and Automation*, Philadelphia, PA, 2022.